

渗铝及扩散处理对电弧喷涂层结合强度的影响

王 强, 兰冬云, 宣兆志, 刘成会

(吉林大学 材料科学与工程学院, 长春 130025)

摘 要: 利用电弧喷涂技术、渗铝和扩散处理工艺, 在铸铁表面制作了具有微冶金结合的18-8不锈钢耐热耐蚀涂层。采用光学显微镜、SEM及X射线衍射等方法, 对经过不同渗铝和扩散处理工艺得到的涂层的组织形貌、相结构及成分进行了分析研究。并采用热疲劳试验对渗铝和扩散处理后涂层的结合强度进行评价。结果表明, 通过渗铝和扩散处理, 涂层与基体之间产生了微冶金结合, 涂层的结合强度得到了显著提高。并且渗铝时间过长不利于提高涂层结合强度, 应合理控制渗铝时间。

关键词: 电弧喷涂; 渗铝; 扩散处理; 结合强度

中图分类号: TG111.6 **文献标识码:** A **文章编号:** 0253-360X(2007)10-061-04



王 强

0 序 言

铸铁是在工业工程中使用最多的几种金属材料之一, 而在高温环境中工作的铸铁常因形成氧化皮、发生生长及形成裂纹而破坏^[1]。改变铸铁基体组织和添加合金元素的做法虽然在一定程度上增强了耐热铸铁的抗氧化能力及抗生长性, 但是效果并不十分理想。而且这样做改变的是整个铸铁件, 而在实际应用中只是要求铸铁件表面附近具有好的耐热耐蚀性, 上述研究方法会造成不必要的浪费, 从而增加生产成本。因此, 在铸铁件表面喷涂上一层耐热耐蚀涂层可使其达到良好的耐热和耐蚀性能。

电弧喷涂技术具有涂层质量好、工件变形小、生产效率高、能源利用率高、经济效益好、操作简单等显著优点, 但电弧喷涂涂层与基体的结合多为机械结合, 从而得到的结合强度并不能令人满意^[2]。实际应用中, 喷涂件常因涂层产生裂纹或脱落而失效。因此, 设法提高涂层的结合强度成为急需解决的问题之一。

对电弧喷涂涂层结合强度的研究在国内外已经有相关单位和个人在进行这方面的工作, 但多是从电弧喷涂工艺参数及焊丝的选用上考虑, 这样得到喷涂层在某些性能上还不尽如人意, 例如热疲劳性能差, 并且得到的电弧喷涂涂层结合强度的提高有限。文中采用渗铝^[3,4]和扩散处理^[5,6]新工艺方法, 使涂层与基体产生微冶金结合, 从而显著地提高电弧喷涂层的结合强度。

1 试 验

为了进行对比试验总共制备了三类试件。试验基材选用尺寸为40 mm×40 mm×6 mm的铸铁件, 表面经喷砂, 然后进行电弧喷涂。

不同类型试件的制备如下, 第一类试件在进行电弧喷涂前先进行渗铝处理, 即将基材置于700℃的铝液中浸泡不同时间, 按渗铝时间30, 60, 90和120 min可将试件标号为A1, A2, A3和A4, 渗铝结束后进行电弧喷涂, 在基材表面喷涂上一层18-8不锈钢涂层, 然后在试件进行扩散处理; 第二类试件进行两次电弧喷涂, 首先在基材上喷涂一层铝作为过渡层, 然后再在过渡层上喷涂上一层18-8不锈钢涂层作为外层, 喷涂结束后进行扩散处理, 试件标号为S; 第三类试件与第二类试件具有同样的过渡层和外层涂层, 但不进行扩散处理, 试件标号为D。

电弧喷涂过程的喷涂距离为100 mm, 喷涂气压为0.7 MPa, Al焊丝的直径为 $\phi 3$ mm (Al>99%, Cu<0.5%, Fe<0.3%); 18-8不锈钢焊丝的直径为 $\phi 2.5$ mm (18 Cr, 8 Ni, C<0.1%)。电弧喷涂过程的工艺参数见表1。

扩散处理工艺是将试件放入中温箱式电阻炉中加热到550℃保温1 h, 然后随炉冷却, 炉内升温控制为200℃以下时电流控制为10 A, 以上时电流控制为20 A, 升温过程大约是30 min左右。

通过热疲劳试验测定涂层的结合强度, 热疲劳试件尺寸为20 mm×15 mm×6 mm, 并且根据表1中

表 1 电弧喷涂工艺参数
Table 1 Arc spraying parameters

| 试件 | Al 层 厚度 d_1/mm | 喷涂 电压 U_1/V | 喷涂 电流 I_1/A | 18-8 不 锈钢层 厚度 d_2/mm | 喷涂 电压 U_2/V | 喷涂 电流 I_2/A | 涂层 厚度 d/mm |
|----|-------------------------------|----------------------------|----------------------------|--|----------------------------|----------------------------|---------------------------|
| A1 | — | — | — | 0.49 | 28 | 300 | 0.49 |
| A2 | — | — | — | 0.51 | 28 | 300 | 0.51 |
| A3 | — | — | — | 0.49 | 28 | 300 | 0.49 |
| A4 | — | — | — | 0.50 | 28 | 300 | 0.50 |
| S | 0.11 | 24 | 200 | 0.40 | 27 | 420 | 0.51 |
| D | 0.13 | 24 | 200 | 0.39 | 27 | 420 | 0.52 |

的试件制备而来, 标号不变。热疲劳试验在热疲劳试验机上进行, 试件在炉内温度为650 ℃的炉腔内保温12 s后快速淬入水中冷却3 s, 一个循环时间为25 s。如此循环, 每 100 次记录试件涂层状况。

用 XR—6 型光学金相显微镜和 JSM—5500LV 型扫描电镜 (SEM) 观察涂层试件横截面的显微组织。用 D/max 2500 pc 型 X 射线衍射仪对涂层进行相组成分析和成分分析, 衍射条件为 $\text{CuK}\alpha$, 40 kV 和 100 mA。

2 试验结果与讨论

2.1 热疲劳试验

热疲劳试验结果见表 2。通过热疲劳试验结果可以看出, 经过渗铝处理的试件可承受的热疲劳次数均比未经渗铝的试件多, 而且经过扩散处理的试件可承受的热疲劳次数又比未经扩散处理的试件多, 从而说明了渗铝和扩散处理工艺可显著提高涂层的结合强度。从表 2 中还可看出, 不同渗铝时间的渗铝试件可承受的热疲劳次数也不相同, 渗铝1 h 的试件承受的次数多, 这说明了渗铝时间需进行控制, 合适的渗铝时间更有利提高涂层的结合强度。

表 2 热疲劳试验结果
Table 2 Results of thermal fatigue tests

| 试件 | 热疲劳试验次数 | | | | | | |
|----|---------|----------|-------|----------|----------|----------|-------|
| | 1 200 | 3 100 | 4 000 | 5 000 | 5 500 | 6 000 | 6 500 |
| A1 | — | — | — | 产生 裂纹 | 少量 脱落 | — | — |
| A2 | — | — | — | — | — | — | 完好 |
| A3 | — | — | — | — | — | 产生 裂纹 | — |
| A4 | — | — | — | — | — | 产生 裂纹 | — |
| S | — | 产生 裂纹 | 脱落 | — | — | — | — |
| D | 脱落 | — | — | — | — | — | — |

基体与涂层之间产生大量的微冶金结合可以极大地提高涂层的结合强度。通过促使基体与涂层之间各种组元的大量扩散以至使其之间产生扩散相变, 可在基体与涂层之间得到大量金属间化合物^[7], 从而实现微冶金结合。为了研究涂层和基体之间的扩散, 根据菲克第一定律(1)和菲克第二定律(2)^[8]和扩散系数公式(3), 即

$$J = -D \frac{\partial C}{\partial x}, \tag{1}$$

$$\frac{\partial C}{\partial t} = D \left(\frac{\partial^2 C}{\partial x^2} \right), \tag{2}$$

$$D = D_0 e^{-\frac{Q}{RT}}, \tag{3}$$

式中: C 为扩散物质的体积浓度; x 为扩散距离; J 为扩散通量; D 为扩散系数; D_0 为扩散常数; t 为扩散时间; e 为自然对数; T 为扩散温度; Q 为扩散激活能; R 为阿弗加德罗常数。

由上述三个公式可见, 提高扩散温度和延长扩散时间可促进扩散的进行。扩散处理工艺改变的就是这两个参数, 通过高温保温一定时间使基体与涂层之间产生大量的物质扩散, 从而提高涂层结合强度。

纯组元之间发生相变需要的条件较高, 且不易发生。在已有部分铁铝间化合物时相变容易发生, 根据 Fe—Al 二元相图(图 1)可见相变的条件需求也不高^[9, 10]。渗铝工艺可在进行电弧喷涂之前先在基体上产生大量金属间化合物, 然后进行电弧喷涂, 在电弧喷涂过程中, 由于熔滴残余热量使基体与涂层交界处温度提高有限, 相变产生困难, 但是在基体表面已有铁铝金属间化合物时铁铝间相变可在较低的温度下进行, 最后在扩散处理过程中由于扩散大量进行引起的相变就更多了。在扩散处理过程中由于扩散大量进行引起的相变就更多了。大量金属间化

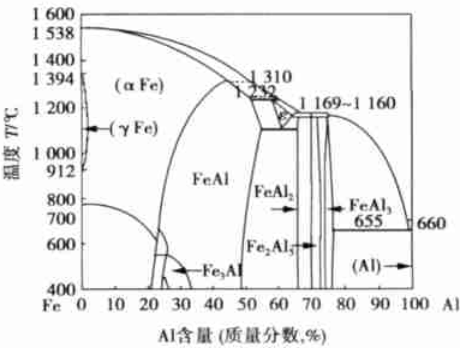


图 1 Fe—Al 二元相图
Fig. 1 Fe—Al binary phase diagram

合物的产生使基体与涂层之间出现了大量的微冶金结合, 这样具有微冶金结合的涂层的结合强度得以显著提高。但是, 渗铝时间不同在基体表面上出现的铁铝化合物是不同的, 长时间的渗铝会在基体表面出现 FeAl_2 , FeAl_3 和 Fe_2Al_5 相, 这些相是硬脆相, 它们的存在对结合强度是不利的^[4]。因此, 渗铝时间不易太长, 应在硬脆相未出现或少量出现时结束渗铝。

2.2 成分分析及显微组织

图 2 为 A4 试件的基体与涂层的界面处的 X 射线衍射图。从图中看出在界面处存在大量的铁铝化合物, 包括 FeAl , Fe_3Al , FeAl_2 和 Fe_2Al_5 。其中, FeAl 和 Fe_3Al 的含量较多, FeAl_2 和 Fe_2Al_5 含量较少。这些铁铝化合物的存在证实了涂层和基体的结合是微冶金结合, 从而提高了涂层的结合强度, 但同时硬脆相的存在又对涂层结合强度不利, 致使 A4 试件的涂层结合强度不是很高。因此渗铝时间不易过长。

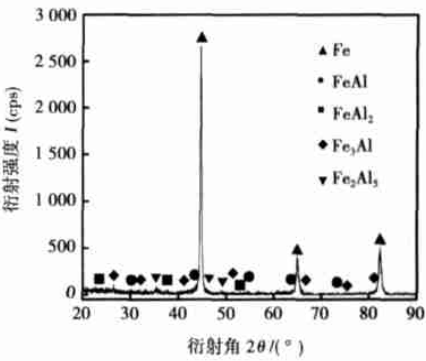


图 2 A4 试件涂层与基体界面的 X 射线衍射图
Fig.2 XRD pattern of interface between coatings and substrates of A4 specimen

用光学显微镜对试件的横截面进行了组织观察, 见图 3。

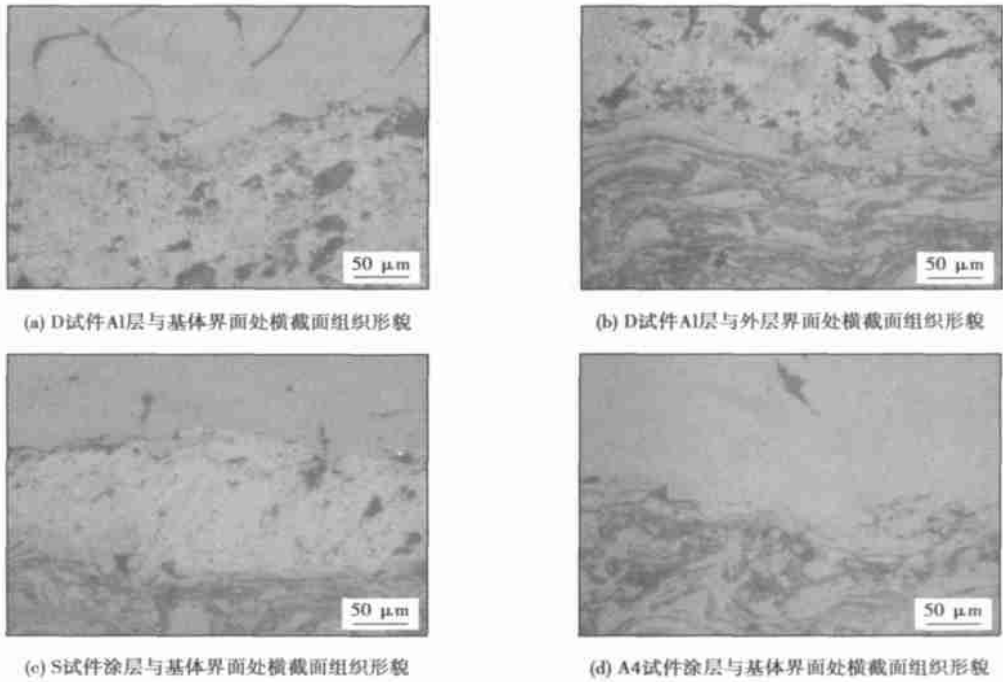


图 3 不同处理工艺制备的涂层与基体界面处横截面组织
Fig.3 Cross section morphologies of interfaces of coatings and substrates of specimens with different processes

图 3c 是 S 试件经过扩散处理后涂层与基体界面处横截面组织形貌图, 可以看出经过扩散处理工艺后的试件涂层出现向基体生长的趋势, 而且涂层的状况得以改善, 孔隙变小变少, 这些都能提高涂层的结合强度。比较图 3a, b, c, 可以看出扩散处理工艺可以促进基体与涂层之间各组元的扩散, 以至在基体与涂层的界面处出现微冶金结合, 从而显著提

高涂层的结合强度。
图 3d 显示的经过渗铝的 A4 试件横截面的显微结构, 图中涂层与基体界面处变得模糊, 部分地方出现融合现象, 这种融合现象的出现表明了此处出现微冶金结合, 从而涂层的结合强度得以提高。图 4 是试件 A2 的涂层与基体交接处横截面的 SEM 组织形貌图, 从中可以看出部分地方有融合现象, 而且涂

层有向基体内部生长的趋势。这种组织形貌证实了渗铝和热处理工艺对涂层结合强度的影响,说明渗铝和热处理工艺可有效地提高涂层的结合强度。

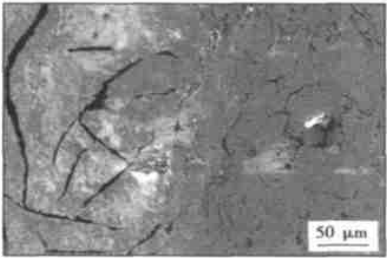


图 4 A2 试件涂层与基体界面处横截面 SEM 图
Fig. 4 SEM morphology of cross-section of interface of coatings and substrates of A2 specimen

3 结 论

- (1) 渗铝及扩散处理工艺可以促进基体与涂层之间各组元的扩散和金属间相变的产生,以至在基体与涂层的界面处产生大量的金属间化合物,进而在基体与涂层的界面处出现微冶金结合,从而显著提高涂层的结合强度。
- (2) 渗铝时间过长会在基体表面上产生硬脆相,对涂层的结合强度不利,因此渗铝时间不易过长,1 h 是一个比较理想的时间。

参考文献:

[1] 徐滨士,朱绍华.表面工程与维修[M].北京:机械工业出版社,1996.

[2] Gedzevicius I, Valulis A V. Analysis of wire arc spraying process variables on coatings properties[J]. Journal of Materials Processing Technology, 2006, 175(1-3): 206-211.

[3] Sharafi S, Farhang M R. Effect of aluminizing on surface microstructure of an HH309 stainless steel[J]. Surface and Coatings Technology, 2006, 200(16-17): 5048-5051.

[4] Shigeaki Kobayashi, Takao Yakou. Control of inter metallic compound layers at interface between steel and aluminum by diffusion-treatment [J]. Materials Science and Engineering: A, 2002, 338(1-2): 44-53.

[5] 崔国文. 缺陷、扩散与烧结[M]. 北京:清华大学出版社,1990.

[6] 何 鹏,张九海.相变扩散连接界面生成金属间化合物的数值模拟[J].焊接学报,2000,21(3):75-78.

[7] 何康生,曹雄夫.异种金属焊接[M].北京:机械工业出版社,1986.

[8] 赵 品,谢辅洲,孙枕国.材料科学基础教程[M].哈尔滨:哈尔滨工业大学出版社,2002.

[9] 尹衍升,施忠良,刘俊友.铁铝金属间化合物[M].上海:上海交通大学出版社,1996.

[10] Kattner U R, Massalski T B. Binary alloy phase diagrams[M]. Material Park: ASM International, 1990.

作者简介:王 强,男,1954 年出生,教授。主要从事传统金属材料改性研究。发表论文 50 余篇。
Email: drqwang@sina.com.cn

high-temperature tensile test; endurant tensile test

Welding process of micro-alloying cast iron electrode ZHAI Qiuya, ZHAI Bo, TANG Zhen, XU Jinfeng (School of Materials Science and Engineering, Xi'an University of Technology, Xi'an 710048, China). p53—56

Abstract: Using a micro-alloying cast iron electrode the relationship between preheat temperature and microstructure and properties of joint were investigated by backing welding with low-current and then continuous welding with high-current. The results showed that the micro-alloying cast iron electrode has strong graphitizing ability and the weld metal had a little chilling tendency. The applied welding process can effectively decrease the depth of fusion zone and suppress the precipitation of cementite in fusion zone at a great extent. Thus the welding with the micro-alloying cast iron electrode can be realized at ambient temperature. When the preheated temperature is less than 200 °C, the homogeneous weld can be obtained which has the same microstructure and properties as base metal. With the increase of the preheat temperature, the graphite morphology in weld changes from spotted graphite to rosette graphite to flake graphite. The contents of graphite and ferrite increase while the hardness of the weld decreases. If the preheated temperature reaches to 200 °C, the microstructure of the weld consists of pearlite, ferrite, flake graphite and rosette graphite, and the microstructure of fusion zone consists of pearlite, small shiver ferrite and undercooled graphite. The welded joint has excellent mechanical properties.

Key words: micro-alloying cast iron electrode; iron casting; ambient temperature welding; microstructure and properties of joint

Analysis of characteristic of vertical position laser welding for aluminum alloys MIAO Yugang, CHEN Yanbin, LI Lijun, WU Lin (State Key Laboratory of Advanced Welding Production Technology, Harbin Institute of Technology, Harbin 150001, China). p57—60

Abstract: The experiments of vertical and flat position laser welding for 4 mm-thick 5A06 aluminum alloys were implemented, and the characteristics of weld dimension and porosity in the vertical position laser welding for aluminum alloys were investigated. The results show that the concave value and excessive penetration value of vertical welding is less than those of flat welding. Further, with the increase of heat input, the difference of vertical and flat welding becomes obvious. The weld appearance and dimension of the vertical welding and flat welding were slightly different. When the heat input is increased to a great extent, the weld depth of vertical welding is more than that of flat welding. However, the weld width of vertical welding is less than that of flat welding. The porosity of vertical position laser welding for aluminum alloys is composed of the large and irregular porosity or hole. It is not obviously different during vertical welding and flat welding, and a great deal of porosity concentrates in the upper and middle part of weld section, which can be indicated from the distributing position and shape of porosity. The number of porosity in vertical welding was slightly less than that of flat welding for the same welding parameters.

Key words: aluminum alloys; vertical position laser welding; flat welding; characteristic

Effect of aluminizing and diffusion treatment on adhesive strength of arc sprayed coatings WANG Qiang, LAN Dongyun, XUAN Zhaozhi, LIU Chenghui (College of Materials Science and Engineering, Jilin University, Changchun 130025, China). p61—64

Abstract: Corrosion-resisting and heat-resisting coatings of 18-8 stainless steel were made by arc spraying, aluminizing and diffusion treatment on cast iron. The microstructures and chemical compositions of coatings with aluminizing and diffusion treatment were studied by optical microscope, scanning electron microscope and X-ray diffraction. And the adhesive strength of coatings was evaluated by thermal fatigue tests. The results show that there are some regions with metallurgy bonding on the interface between coatings and substrates through aluminizing and diffusion treatment, therefore, the adhesive strength of coatings were improved greatly. And a long period of aluminizing time is adverse to the adhesive strength of coatings, so aluminizing time should be controlled well.

Key words: arc spraying; aluminizing; diffusion; adhesive strength

Microstructure and melting property of Sn-2.5Ag-0.7Cu-XGe solder MENG Gongge¹, YANG Tuoyu², CHEN Leida¹ (1. School of Material Science & Engineering, Harbin University of Science and Technology, Harbin 150040, China; 2. Anhui Science and Technology University, Bengbu 233100, Anhui, China). p65—68

Abstract: The 3 composition Sn-2.5Ag-0.7Cu-XGe lead-free solders were studied by scanning electron microscope and differential scanning calorimetry equipments. The result indicates that the microstructure is cobblestone-like pro-eutectic grain and scattered long narrow piece and small pellet eutectic mixture. With 0.5% or 1.0% element Ge, the microstructure morphology does not change. But the intermetallic compounds of Ag₃Sn and Cu₆Sn₅ tend to be fine, and their dispersion tends to be well-distributed, and Ag₃Sn phase tends to be fine needle from long narrow piece. By adding element Ge, the temperatures of the melting beginning, the melting peak and the melting finish all reduce correspondingly. And in the melting curve, the endothermic peak changes is narrow, and the melting finish part is long, but the melting temperature zone varies a little.

Key words: lead-free solder; microstructure; melting property

Solidification cracking mechanism of 690 nickel-based alloy surfacing metal BO Chunyu, YANG Yuting, CHOU Shuguo, ZHOU Shifeng (Harbin Welding Institute, China Academy of Machinery Science and Technology, Harbin 150080, China). p69—72

Abstract: Transverse restraint test was used to investigate the solidification cracking mechanism of 690 nickel-based alloy surfacing metal. Results show that the solidification cracking susceptibility of 690 nickel-based alloy surfacing metal is closely correlated with the segregation process during welding, which is greatly influenced by Nb. The solidification temperature of 690 nickel-based alloy surfacing metal falls when the Ni, Nb-rich phases segregate on the grain boundary or subgrain boundary, which induces that the ductility decreases and the appearance is fined. Then, cracking initiates and